

# **Influence of Target Concentration and Background Binding on *In Vitro* Selection of Affinity Reagents**

Jinpeng Wang<sup>a</sup>, Joe F. Rudzinski<sup>b</sup>, Qiang Gong<sup>a,c</sup>, H. Tom Soh<sup>a,c\*</sup>, Paul J. Atzberger<sup>a,b\*</sup>,

<sup>a</sup>*Department of Mechanical Engineering, University of California, Santa Barbara, CA, 93106, USA*

<sup>b</sup>*Department of Mathematics, University of California, Santa Barbara, CA, 93106, USA*

<sup>c</sup>*Materials Department, University of California, Santa Barbara, CA, 93106, USA*

To whom correspondence should be addressed. Email:  
[atzberg@math.ucsb.edu](mailto:atzberg@math.ucsb.edu) and [tsoh@engr.ucsb.edu](mailto:tsoh@engr.ucsb.edu)

---

## **Abstract**

Nucleic acid-based aptamers possess many useful features that make them a promising alternative to antibodies and other affinity reagents, including well-established chemical synthesis, reversible folding, thermal stability and low cost. However, the selection process typically used to generate aptamers (SELEX) often requires significant resources and can fail to yield aptamers with sufficient affinity and specificity. A number of seminal theoretical models and numerical simulations have been reported in the literature offering insights into experimental factors that govern the effectiveness of the selection process. Though useful, these previous models have not considered the full spectrum of experimental factors or the potential impact of tuning these parameters at each round over the course of a multi-round selection process. We have developed an improved mathematical model to address this important question, and report that both target concentration and the degree of non-specific background binding are critical determinants of SELEX efficiency. Although smaller target concentrations should theoretically offer superior selection outcome, we show that background binding levels dramatically affect the target concentration that will yield maximum enrichment at each round of selection. Thus, our model enables experimentalists to determine appropriate target concentrations as a means for protocol optimization. Finally, we perform a comparative analysis of two different selection methods over multiple rounds of selection, and show that methods with inherently lower background binding offer dramatic advantages in selection efficiency.

## Introduction

Relative to other commonly used affinity reagents, nucleic acid-based aptamers possess many useful features including chemical synthesis, reversible folding, thermal stability and low cost, making them a promising alternative to antibodies and other protein-based reagents [1–3]. To date, DNA or RNA aptamers have been generated for a wide variety of molecular targets including proteins[4], small molecules[5], cell surfaces[6,7], and even whole organisms [8]. Aptamers are typically isolated from combinatorial oligonucleotides libraries via a method of selection called Systematic Evolution of Ligands by EXponential enrichment (SELEX), which entails an iterative process of nucleic acid binding, separation and amplification (**Fig. 1**) [9,10]. In SELEX, a large population of nucleic acid molecules is chemically synthesized wherein each molecule contains random sequences that are able to adopt unique conformations through intramolecular binding. Candidate molecules are selected for their ability to specifically bind to a chosen target, and selected molecules are amplified to create more copies. The cycle of selection and amplification is repeated to successively enrich aptamers with high affinities. Though conceptually simple, SELEX is time-consuming and resource-intensive and does not always yield reagents with desired characteristics. For example, when one tabulates the affinity of DNA aptamers for protein targets in literature, one observes a large variability spanning six orders of magnitude[11]. Multiple factors contribute to this large variability, including the structure and charge state of the target, design and complexity of the library, as well as a variety of experimental factors in selection and measurement.

To gain insights into those experimental factors that can influence SELEX, a number of investigators have developed theoretical models and performed numerical simulations of the selection process[12–16]. For example, seminal work by Irvine, Tuerk and Gold performed an extensive mathematical analysis of selection to investigate how experimental conditions such as target concentration, background binding, and partitioning efficiency of high-affinity aptamers can affect the selection [12]. Building on these results, Levine and Nilsen-Hamilton provided sufficient conditions and related theorems to show the circumstances under which selection is ensured to converge to the optimal molecule within the library[15]. Furthermore, to investigate the role of the discrete number of molecules undergoing selection, Waterman and coworkers developed a probabilistic model to study the link between the number of target molecules and the number of PCR amplification cycles performed on the probability of achieving

convergence to the best molecule within the library[17]. However, these various investigations have not explored how other important experimental conditions, such as tuning the round-to-round target concentration and background binding level, can exert their effect over multiple rounds of a SELEX experiment.

To address this important issue, we have performed a mathematical analysis of the critical experimental conditions that can influence the affinity distribution of the selected aptamer pool. Based on these data, we developed a model that uses the binding characteristics of a given library or aptamer pool and the non-specific background binding level associated with particular SELEX conditions to determine the ideal target concentration for optimal selection of high affinity aptamers in each SELEX round. We also used our model to compare two different SELEX methods, with low and high levels of background binding. We show that under low-background conditions, high selection stringency can be applied to achieve rapid convergence of the library to the highest affinity aptamer, whereas the high-background method limits the maximal enrichment at each round, requiring more selection rounds to achieve convergence. Interestingly, enrichment in the low-background method depends less sensitively on target concentration to achieve optimal enrichment. In contrast, the greater sensitivity associated with the high-background method means that a considerably narrower range of target concentration is required to attain efficient selection, necessitating tighter control of experimental conditions.

# Methods

## Mathematical Model for SELEX

### Chemical Kinetics

In our notation,  $[A_i]$  denotes the concentration of unbound aptamers of type  $i$  and  $[S]$  denotes the concentration of unbound target molecules. The concentration of target-bound aptamers is denoted by  $[A_iS]$  for aptamers of type  $i$ , as shown in Figure 1.

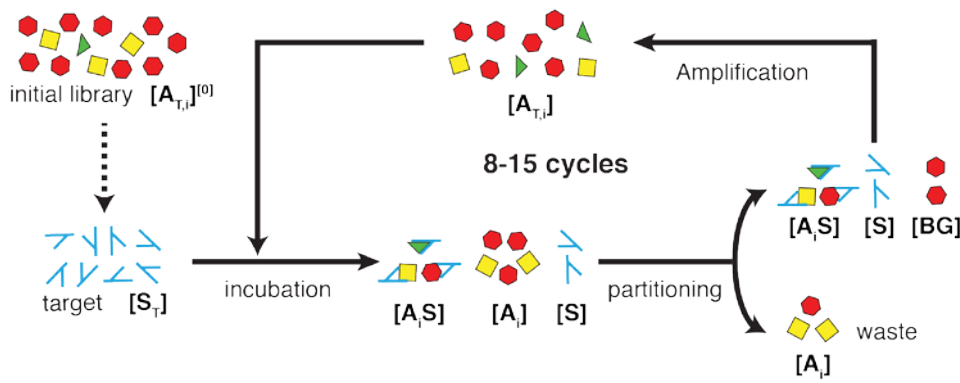
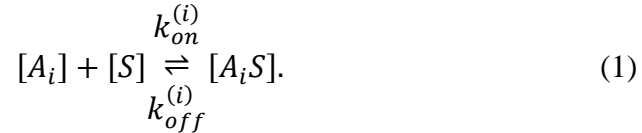


**Figure 1. SELEX scheme for selecting high affinity aptamers.** The target molecules and aptamer library are incubated and then partitioned to separate unbound and target-bound aptamers. Selected aptamers are amplified via polymerase chain reaction (PCR) to create an enriched pool for use in the next round of selection. Typically, 8-15 rounds of selection are required to isolate aptamers with high affinities. In our model,  $[A_i]$  denotes the concentration of unbound aptamers of type  $i$  and  $[S]$  denotes the concentration of unbound target molecules. The concentration of target-bound aptamers is denoted by  $[A_iS]$  for aptamers of type  $i$ .

The binding and unbinding kinetics are modeled by



$k_{on}^{(i)}$  denotes the association rate for an aptamer binding available free target molecules, and  $k_{off}^{(i)}$  denotes the dissociation rate for that aptamer from the target molecule. In our analysis, we assume a Langmuirian 1:1 interaction, in which only one aptamer molecule may bind to a single target molecule.

The rate of change of the concentration of aptamer-target complexes is given by

$$\frac{d[A_iS]}{dt} = k_{on}^{(i)} \cdot [A_i] \cdot [S] - k_{off}^{(i)} \cdot [A_iS] \quad (2)$$

The total concentration of target is given by

$$[S_T] = [S] + \sum_i [A_iS]. \quad (3)$$

The total concentration of aptamers of type  $i$ , both bound and unbound, is given by

$$[A_{T,i}] = [A_i] + [A_iS]. \quad (4)$$

The total target concentration given in equation (3) and the total aptamer concentration given in equation (4) are conserved quantities that remain constant throughout each round of selection. The aptamer-target dissociation constant for aptamers of type  $i$  is denoted by

$$k_d^{(i)} = \frac{k_{off}^{(i)}}{k_{on}^{(i)}}. \quad (5)$$

#### ***Steady -State after Incubation Step***

Each selection step of SELEX entails the collection of aptamers from the starting library that are bound to target molecules. To model this aspect of SELEX and the population of bound aptamers, we assume that the reactions of the system during this incubation step reach equilibrium. In this case, the concentration of free and bound aptamers is given by the steady-state of the kinetic equation (2). Under these assumptions, and following an approach similar to [15], an implicit equation for the steady-state concentrations can be obtained in terms of unbound free target as

$$[S] \left( 1 + [A_T] \sum_i \frac{F_i}{k_d^{(i)} + [S]} \right) = [S_T]. \quad (6)$$

In equation (6), the fraction of type  $i$  aptamers in the library is denoted by

$$F_i = \frac{[A_{T,i}]}{[A_T]}. \quad (7)$$

From the steady-state of equation (2), the dissociation constant of type  $i$  aptamers can be expressed as

$$k_d^{(i)} = \frac{[A_i][S]}{[A_iS]}. \quad (8)$$

The target bound aptamer concentration can be expressed as

$$[A_iS] = \frac{[S][A_{T,i}]}{k_d^{(i)} + [S]}. \quad (9)$$

This is obtained by letting equation (2) be equal to zero and using equation (4) and (5).

To characterize this population, it is useful to define a bulk equilibrium dissociation constant  $\bar{k}_d$  for the pool of aptamers, similar to the conventional definition of the dissociation constant  $k_d$

$$\bar{k}_d = \frac{[A][S]}{[AS]}. \quad (10)$$

$[A]$  denotes the concentration of unbound free aptamers and  $[AS]$  denotes the total concentration of bound aptamers irrespective of type. This allows for the bound aptamer concentration to be expressed as

$$[AS] = \frac{[S][A_T]}{\bar{k}_d + [S]}, \quad (11)$$

where

$$[A_T] = [AS] + [A]. \quad (12)$$

#### ***Model for Selection without Background Binding***

Each round of SELEX produces a new aptamer pool. In the ideal case, in which only aptamers specifically bound to target are recovered, the new pool of aptamers is described based on our analysis above by

$$\begin{aligned} B_i &= \frac{[A_i S]}{[AS]} = \frac{\frac{[S][A_{T,i}]}{k_d^{(i)} + [S]}}{\sum_j \frac{[S][A_{T,j}]}{k_d^{(j)} + [S]}} = \frac{F_i}{F_j} \cdot \frac{\frac{1}{k_d^{(i)} + [S]}}{\sum_j \frac{1}{k_d^{(j)} + [S]}} = \left[ \sum_j \frac{k_d^{(i)} + [S]}{k_d^{(j)} + [S]} \left( \frac{F_j}{F_i} \right) \right]^{-1} \\ &= \frac{F_i}{k_d^{(i)} + [S]} \cdot \left[ \sum_j \frac{F_j}{k_d^{(j)} + [S]} \right]^{-1} \end{aligned} \quad (13)$$

$B_i$  denotes the fraction of type  $i$  aptamers in the newly selected aptamer pool.  $F_i$  denotes the fraction of type  $i$  aptamers in the initial library subject to selection, as defined in equation(7). By using the bulk dissociation constant of the library  $\bar{k}_d$ , defined by equation (10), and combining equations(9) and (10), the fraction of type  $i$  aptamers  $B_i$  can be simplified and expressed as

$$B_i = \frac{\bar{k}_d + [S]}{k_d^{(i)} + [S]} F_i. \quad (14)$$

From equation(14) the successive aptamer distributions after a round of selection can be expressed as

$$B_i^{[n+1]} = \frac{B_i^{[n]}}{k_d^{(i)} + [S]} \cdot \left[ \sum_j \frac{B_j^{[n]}}{k_d^{(j)} + [S]} \right]^{-1} = \frac{\bar{k}_d^{[n]} + [S]}{k_d^{(i)} + [S]} B_i^{[n]}. \quad (15)$$

The round of selection is denoted by the superscript  $n$ . From Equation (15),  $\bar{k}_d^{[n]}$  is given by

$$\bar{k}_d^{[n]} = \left( \sum_i \frac{B_i^{[n]}}{k_d^{(i)} + [S]} \right)^{-1} - [S]. \quad (16)$$

We remark that after a single round of selection, aptamers of type  $i$  with dissociation constants larger than  $\bar{k}_d$  will comprise a smaller fraction of the new pool (since the prefactor multiplying  $F_i$  will be less than one) and those with dissociation constants smaller than  $\bar{k}_d$  will be enriched and comprise a greater fraction of the new pool (since the prefactor multiplying  $F_i$  will be greater than one). The target concentration is a central experimental parameter that can be readily varied during the SELEX experiment. Based on this model, a smaller target concentration should yield a smaller unbound free target concentration  $[S]$  during SELEX.

#### ***Model for Selection with Background Binding***

In the above analysis, we assumed that all aptamers not bound to target are removed during the partitioning step of SELEX. However, in practice, the purification process is not ideal, and a fraction of unbound and non-specifically bound aptamers will be present in the selected pool. These constitute the background aptamers (BA). To model such experimental realities more accurately, we consider the effect of BA on the SELEX process.  $[A_i S]_p$  denotes aptamers of type  $i$  that are captured during the partitioning step.

We model the background contributions to partitioning similarly to [15] by

$$[A_i S]_p = [A_i S] + ([A_{T,i}] - [A_i S]) \cdot BG. \quad (17)$$

BG is the fraction of BA of type  $i$  that are recovered during partitioning. We remark that  $[A_i S]_p$  includes both the aptamers specifically bound to targets as well as the BA. The fraction of type  $i$  aptamers that appear in the new pool after a round of selection is given by

$$B_{i,bg} = \frac{[A_i S]_p}{\sum_j [A_j S]_p} = \frac{(1 - BG)[A_i S] + BG[A_{T,i}]}{(1 - BG)[AS] + BG[A_T]}. \quad (18)$$

This can be expressed as

$$B_{i,bg} = \frac{\left( \frac{[S]}{k_d^{(i)} + [S]} + \frac{BG}{1 - BG} \right)}{\left( \frac{[S]}{\bar{k}_d + [S]} + \frac{BG}{1 - BG} \right)} \cdot F_i. \quad (19)$$

This follows by substituting equations (7) and (9) into equation (18). This shows clearly how the fraction of aptamers of type  $i$  obtained in the new pool is influenced by background binding during selection. We remark that in the case where the limit for BG tends to zero, we recover the expression for pure selection without background (see

equation (14)). In the case where the limit of BG tends to one, we find that background binding results in loss of selective pressure, and the fraction of aptamers of type  $i$  selected in the new pool is equal to the fraction of aptamers of type  $i$  in the previous pool.

### ***Model of the Affinity Distribution in the Initial Random Library***

Aptamer selection begins with a large random combinatorial library of nucleic acids, typically containing up to  $\sim 10^{14}$  molecules. These molecules are expected to have a wide range of affinities to a given target molecule, depending on the specific molecular interactions between an individual aptamer and that target. Important factors contributing to this affinity include aptamer/target charge state, size, structural stability and distribution of cationic/anionic regions [11]. For the library as a whole, it is expected that many different aptamers will have similar affinities for a target. We shall model the library by considering it as a collection of sub-types, with each aptamer grouped into a class according to its affinity as characterised by its equilibrium dissociation constant ( $k_d$ ).

To investigate the *in vitro* selection of aptamers, it is necessary to consider the initial affinity distribution of the combinatorial library for a target of interest. It is commonly hypothesized that the binding free energies ( $\Delta G$ ) between nucleic acids and proteins are normally distributed [13,18]. The binding free energy is related to the equilibrium dissociation constant ( $k_d$ ) by

$$\Delta G = k_B T \cdot \ln(k_d) \quad (20)$$

where  $k_B$  is the Boltzmann constant and  $T$  is the absolute temperature. This makes it natural to consider a log-normal distribution for the equilibrium dissociation constants ( $k_d$ ) of library components. The affinity distribution of library molecules for the target protein has the probability density function

$$p(\ln k_d) = \frac{1}{\sigma\sqrt{2\pi}} e^{-\frac{(\ln k_d - \mu)^2}{2\sigma^2}} \quad (21)$$

To model this log-normal distribution, we use the normal probability density function in with  $\mu$  and  $\sigma$  be -13.1 and 1.07 respectively. This affinity distribution, shown in Figure 2, is consistent with the reported value in the literature [12,13], where the bulk  $k_d$  is in the low  $\mu\text{M}$  range. For our model, we arbitrarily chose a bulk  $\bar{k}_d$  value of 1.25  $\mu\text{M}$  and this affinity distribution is used throughout this work. Furthermore, we define high affinity aptamers (HAA) as those possessing  $k_d < 1 \text{ nM}$  to the target molecule.

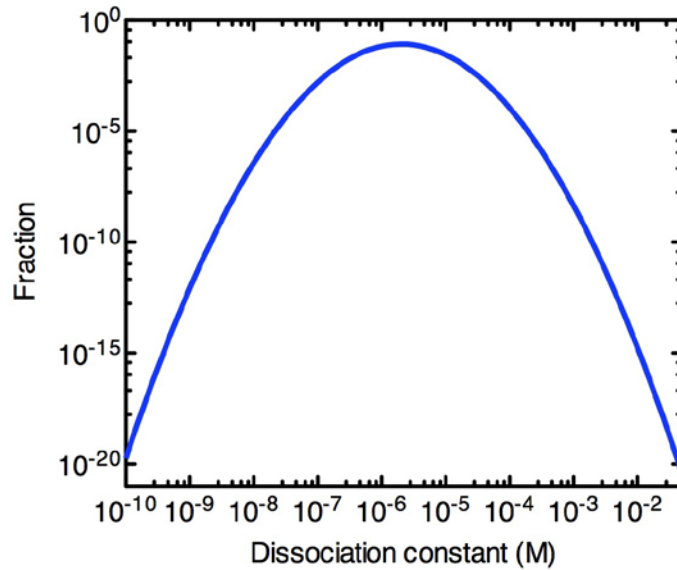


**Figure 2. Affinity distribution of the initial random library.** To model this log-normal distribution, we used a normal probability density function with  $\mu = -13.1$  and  $\sigma = 1.07$ , yielding a bulk  $\bar{k}_d$  of  $1.25 \mu\text{M}$ .

### *Computational Methods*

We modeled the SELEX process by solving a system of non-linear equations having a dimension comparable to the number of different types of aptamers (see equation (9)). To gain quantitative and qualitative insights into the SELEX process, we used numerical methods to compute solutions. Our analysis shows that this high dimensional problem can in fact be reduced to solving only one non-linear. This can be seen by considering equation (6), which involves only one unknown, namely, the unbound free target concentration  $[S]$ . This simplification will be employed throughout our simulation studies. We used Newton iteration to find the solution for  $[S]$ . All of the other concentrations associated with this model can be calculated from  $[S]$  by using equations (3), (4) and (9). By using equation (13), this procedure yields an efficient method to determine the affinity distribution of the new aptamer pool after each round of selection. The bulk dissociation constant  $\bar{k}_d$  can also be readily calculated by using equation (16).

## **Results**

### *Role of Target Concentration without Background Binding*

To analyze the efficiency of each round of selection, we defined the enrichment of

aptamers of type  $i$  as

$$E_i^{[n]} = \frac{B_i^{[n+1]}}{B_i^{[n]}} = \left( 1 + \frac{\bar{k}_d^{[n]} - k_d^{(i)}}{[S]} \right). \quad (22)$$

The superscript  $n$  denotes the round of selection being considered. The enrichment yields the change in the overall affinity distribution of aptamers of type  $I$  between successive rounds of selection.

The target molecule concentration used during the selection process is an important parameter that governs selection pressure. The above model predicts that as the amount of target decreases, the level of HAA enrichment will increase. This suggests that enrichment is greatest when using the lowest feasible target concentration. To investigate the role of target concentration in enrichment and convergence of SELEX, we varied the target concentration over six orders of magnitude, from 1  $\mu$ M to 1 pM. We show a simulation of enrichment of HAA during the first round of selection (Fig.3A) and the fraction of HAA as a function of increasing selection rounds for different target concentrations (Fig.3B). As the target concentration decreases, we found that HAA enrichment changes dramatically - over three orders of magnitude, from 6.6 to 1240 - verifying that the use of low target concentrations can dramatically enhance selection efficiency.

From this analysis, it is tempting to conclude that minimal target concentration should be exclusively used experimentally. However, in practice, other considerations will likely constrain the practical lower limit. Two important predictions of our model are that (i) there is a limit to the maximum enrichment attainable, and (ii) once the target concentration becomes sufficiently small, the additional enhancement from further reduction of target concentration is rather modest. The maximum enrichment achievable is given by the ratio of the bulk dissociation constant  $\bar{k}_d$  and the dissociation constant  $k_d$  associated with HAA,  $E_{max} = \bar{k}_d / k_{d,HAA}$ . Once the target concentration drops below the  $k_d$  of the HAA, further decreases in target concentration have no significant effect. For example, in decreasing the target concentration from 100 pM to 1 pM, we find that the enrichment of HAA increases only slightly, from 1212 to 1240 (Fig. 3A). In this case, the maximum enrichment factor is 1250, indicating that at target concentrations of 100 pM the enrichment is already very close to the theoretical maximum. In general, a useful rule of thumb for the experimentalist is to utilize target concentrations in the range of the  $k_d$  of HAA.

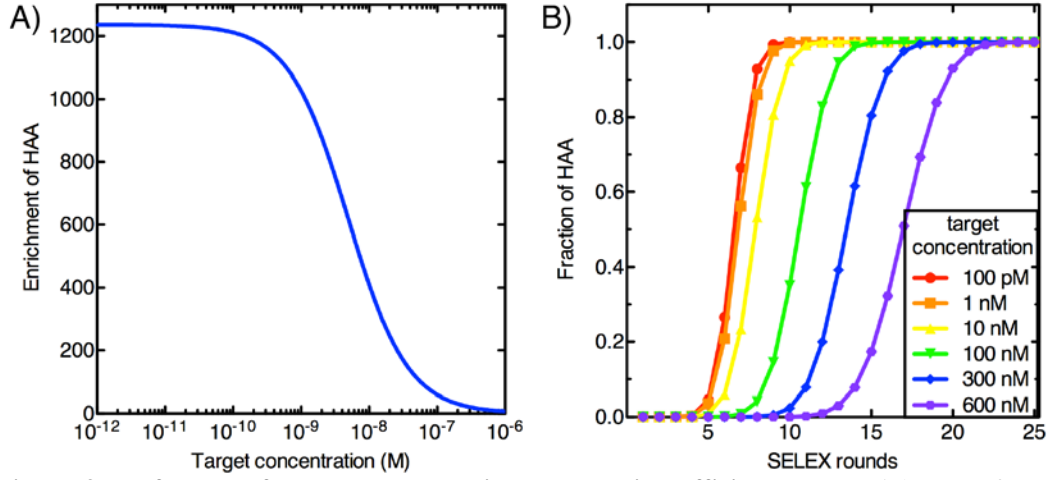


**Figure 3. Influence of target concentration on selection efficiency.**(A) Enrichment of HAA as a function of target concentration. As the target concentration is varied over 6 orders of magnitude, from 1  $\mu$ M to 1 pM, the enrichment of HAA increases from 6.6 to 1240, respectively. (B) The fraction of HAA in the selected pool as a function of selection rounds for varying target concentrations.

### ***Modeling Enrichment with Background Binding***

Another critical practical consideration is the fact that no experimental separation scheme can perfectly partition target-bound molecules from unbound and non-specifically bound background molecules. This is especially important when using extremely low target concentrations, as this background can overwhelm the specifically bound HAA and undermine overall gains to enrichment. Mathematically, the enrichment of HAA in the presence of background aptamers (BA) can be expressed as

$$E = \frac{\sum_i B_{i,bg}}{\sum_i F_i} = \frac{\sum_i \left( \frac{[S]}{k_d^{(i)} + [S]} + \frac{BG}{1 - BG} \right)}{\sum_i \left( \frac{[S]}{\bar{k}_d + [S]} + \frac{BG}{1 - BG} \right)}, \quad (k_d^{(i)} < 1 \text{ nM}). \quad (23)$$

where BG denotes the fraction of BA obtained during partitioning. This uses the results for  $B_{i,bg}$  and  $F_i$  obtained in equation (19). We see that, in contrast to the model without background binding, HAA enrichment no longer increases monotonically as target concentration decreases. This is a consequence of the term involving BG. If the target concentration is too small,  $[S]/(k_d^{(i)} + [S])$  and  $[S]/(\bar{k}_d + [S])$  can become much smaller than  $BG/(1 - BG)$ , so that the enrichment of HAA becomes close to one—meaning no enrichment takes place. Therefore, BG limits the minimum target concentration and maximum enrichment that can be achieved during each round of selection. This makes intuitive sense, and suggests that for a given level of background aptamers, there exists an optimum target concentration that results in the most efficient selection of HAA.

### ***Optimal Target Concentration with Background Binding***

Our model can be used to numerically calculate the target concentration that will achieve the maximum possible enrichment of HAA in the presence of background binding. To quantify the effect of BA on enrichment, we used our model to perform numerical simulations with different BG levels. For target concentrations ranging from 1  $\mu\text{M}$  to 1 pM, we assumed BG ranging from  $10^{-6}$  to  $10^{-2}$ , an experimentally reasonable range [13,19], and calculated the enrichment of HAA using equation (23). The simulation results shown in Figure 4 reveal that when BG is taken into account, the enrichment of HAA differs markedly from the case without BG. As BG increases, maximum enrichment of HAA decreases and occurs at a higher target concentration. For example, when  $\text{BG} = 10^{-6}$ , the optimal target concentration is 174 pM, and results in 1153-fold enrichment of HAA. On the other hand, when BG is increased to  $10^{-2}$ , the optimal target concentration becomes 17.4 nM, and yields significantly lower, 61-fold enrichment. Intuitively, this phenomenon can be explained by the fact that at lower BG, lower target concentrations can be applied during the selection without having the BA dominate the pool, leading to greater competition among aptamers to bind to the target. In this way, BG is an extremely important parameter that controls the SELEX process, and experimental methods should be optimized to keep its value to a minimum.

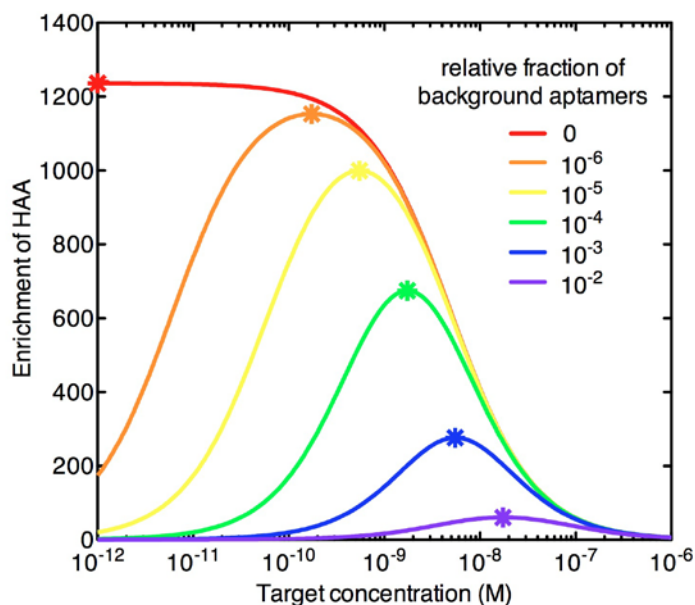


**Figure 4. Effect of background partitioning on selection of high affinity aptamers.** Enrichment of HAA during first rounds of selection is shown as a function of target concentration at different BG levels. The optimal target concentration for maximum enrichment of HAA is shown as (\*). With no

background, the lowest target concentration (1 pM) yields maximum HAA enrichment (1240-fold). As BG rises to  $10^{-6}$ ,  $10^{-5}$ ,  $10^{-4}$ ,  $10^{-3}$  and  $10^{-2}$ , this optimal target concentration increases to 174 pM, 550 pM, 1.74 nM, 5.5 nM and 17.4 nM respectively, yielding diminishing maximum HAA enrichment of 1153-, 999-, 674-, 276- and 60-fold, respectively.

### ***Multiple Selection Rounds with Background Binding***

To gain further insight into the importance of both target concentration and background during selection, we simulated multiple rounds of selection with two different experimental systems. The first mimics microfluidic selection (MF) using magnetic particles, which exhibit low background binding ( $BG \sim 10^{-6}$ ) with the capacity to handle very small amount of target molecules [14,15,18,19]. The second system is modeled after nitrocellulose filter-based separation (NCF), which exhibits relatively high background binding, on the order of  $BG \sim 10^{-2}$  [14,15,16,17]. Next, we simulated a complete SELEX experiment in which six rounds of selection were performed using either method. For each round of selection, we calculated HAA enrichment as a function of target concentration using equation (23) for both methods. Importantly, we used the optimal target concentration for each round, which was numerically calculated from the affinity distribution of the pool generated by the previous round of selection.

We note that the MF method yields significantly higher enrichment of HAA compared to the NCF method (Fig. 5A and B). For example, during the first round of selection, the MF method exhibits HAA enrichment of 1153-fold, ~19 times greater than that achieved by NCF. Importantly, the MF method is also more robust when the target concentration deviates from the optimum, as indicated by shallower slope of the curve near the optimal concentration. For example, in the MF method, a 10-fold deviation in the optimal target concentration in the first round would result in a 20% decrease in the HAA enrichment from 1153- to 910-fold. However, such a deviation in the NCF method would result in a 60% decrease, reducing the HAA enrichment from 61- to 25-fold. In practice, this is a highly useful feature as it offers a significantly larger tolerance for experimental variability.

Over the course of multiple rounds of SELEX, the affinity distributions of the aptamer pools enriched via these two selection methods exhibit interesting differences. In the

MF approach, we observe a uniform shift in affinity distribution from round to round, as BG plays a minimal role (Fig. 5C). On the other hand, interesting distortions in the affinity distribution can be observed in the NCF method, especially in rounds 3, 4 and 5 (Fig. 5D). This is a result of the greater impact of BG, which causes a slow shift in the aptamer population from the low affinity pool (right peak) to the high affinity pool (left peak).

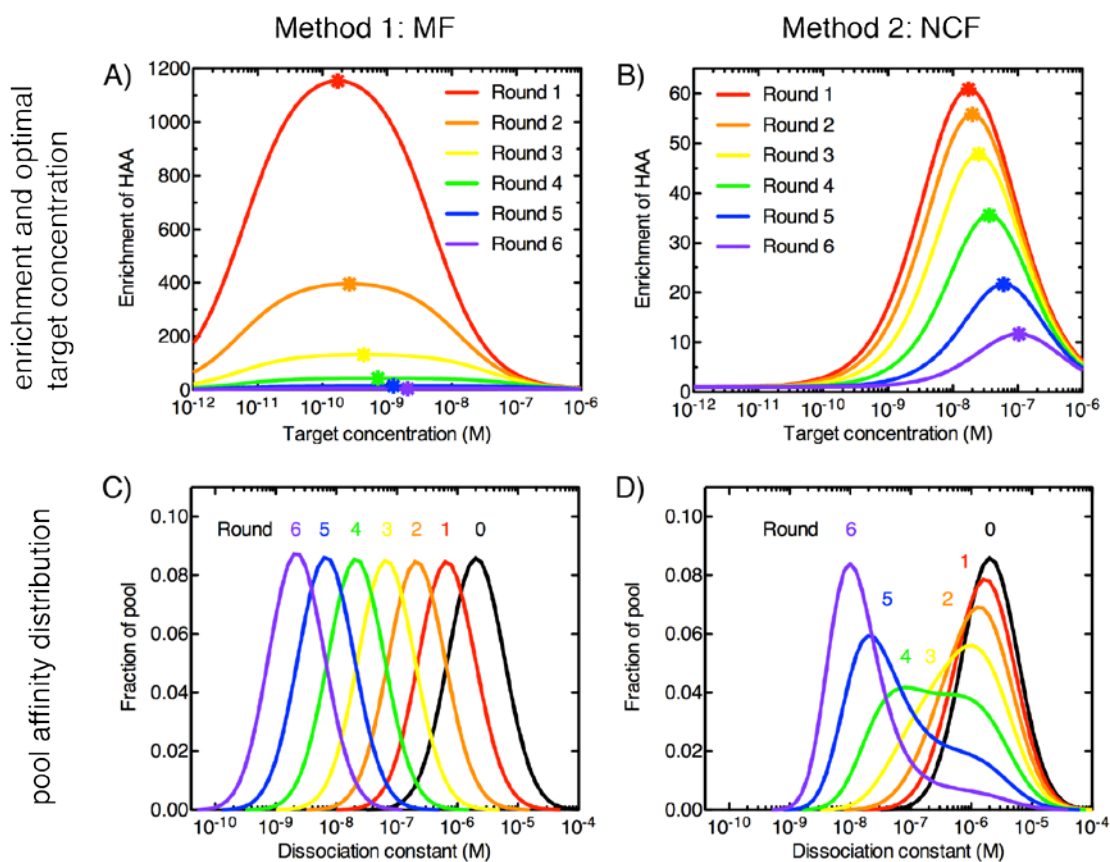


**Figure 5.** Simulations of HAA enrichment during each round of selection via microfluidic (A) or nitrocellulose filter-based SELEX (B) as a function of target concentration. We calculated enrichment using equation (23). Optimal target concentration for achieving maximum enrichment is shown as (\*). These optimal target concentrations were subsequently chosen for each round of SELEX to simulate the new affinity distribution of the selected pool for both microfluidic (C) and filter-based SELEX (D).

Next, using Equation (10), we calculated the bulk  $\bar{k}_d$  for 10 rounds of selection using the two methods. We observe that bulk  $\bar{k}_d$  decreases at a significantly higher rate with MF compared to NCF, ultimately resulting in a pool that exhibits a  $\sim 30$ -fold difference in bulk  $\bar{k}_d$  after ten rounds of simulated selection (Fig. 6A). Finally, we calculated the

fraction of HAA after each round of selection for the two methods. Consistent with the findings shown in Figure 6A, we note that the fraction of HAA increases at a markedly greater rate with MF method compared to NCF (Fig. 6B). For MF, the fraction of HAAs is 25% after 6 rounds, reaches 91% after 8 rounds and saturates at 100% in the 9<sup>th</sup> round. On the other hand, NCF yields a 12% fraction of HAA in the 8<sup>th</sup> round and only reaches 27% after 10 rounds of selection.

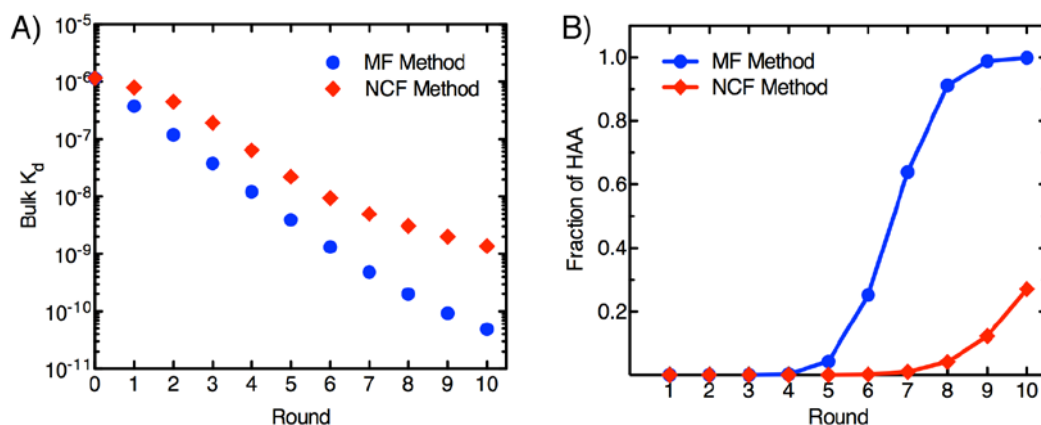


**Figure 6.** Properties of aptamer pools isolated over ten rounds of selection with NCF or MF methods using optimal target concentrations for each round. (A) Bulk dissociation constant ( $k_d$ ) of selected pools after each round of selection. (B) Proportion of HAA at each round of selection. We assume BG of  $10^{-2}$  and  $10^{-6}$  for the MF and NCF methods, respectively.

## Discussion

In this work, we have explored the effect of background binding and target concentration on the outcome of SELEX experiments. We found that minimal target concentrations yield the most efficient selection if one ignores the contaminating effects of non-specifically bound background aptamers. However, this is unrealistic, as practically all methods exhibit background binding at various levels, which represents a competitive presence that can undermine the efficiency gains that would otherwise be achieved at very low target concentrations. Accordingly, we have incorporated this crucial factor into our method for determining selection conditions that will yield the greatest enrichment of high-affinity aptamers. Our model requires two input parameters: background binding, which can be easily obtained experimentally, and the initial bulk affinity distribution, which is commonly described as log-normal distribution. With this

information, our model can calculate the optimal target concentration and predict the affinity distribution of the enriched aptamer pool after each round.

We used our model to characterize two different selection methods: conventional nitrocellulose filter-based SELEX with high background binding, and microfluidic SELEX with low background binding. We found that the range of target concentrations that will yield near-optimal efficiency is heavily dependent on the level of background. This window is very narrow in selection conditions with high levels of background binding, such as NCF. In contrast, the low background binding associated with MF results can tolerate wider range of target concentrations, enabling greater flexibility in experimental design. This finding emphasizes the desirability of reducing background binding as much as possible, not only to achieve more stringent selection pressure by using lower target concentrations, but also to reduce the sensitivity of the convergence of SELEX to the experimental conditions. Our simulations showed that low-background conditions also generate higher-affinity aptamers in fewer rounds. After choosing optimal target concentrations for each round with the two methods, we observed that the bulk dissociation constant decreased at a significantly higher rate for MF, resulting in a pool with a bulk dissociation constant that was ~30-fold lower than that achieved in the pool selected via NCF. Furthermore, six rounds of MF SELEX were sufficient to generate a pool containing a percentage of high-affinity aptamers that could only be achieved after ten rounds of NCF SELEX. Another interesting result is that the optimal target concentration increases as the library becomes more refined. This indicates that even in cases where the optimal target concentration cannot be determined in practice, it is still desirable to use a lower target concentration during initial rounds of selection and then increase this concentration in later rounds. The average dissociation constant of the library can be used as an indicator of the amount by which target concentration should be increased in successive rounds to help enhance the convergence of selection.

This analysis thus provides useful guidelines for designing SELEX experiments with optimized selection conditions. However, we note that the models and analyses presented in this work make a few key assumptions. First, we have used log-normal distribution to describe the aptamer dissociation constants within the initial library. This assumption has been commonly used in previous work [13,18], but to our knowledge has not been experimentally validated. We note that our model can be readily modified to accommodate a different affinity distribution. Second, we assumed a Langmuirian

1:1 interaction between aptamer and target. In reality, multivalent interactions and cooperative binding can occur, whereby more than one aptamer type binds the target molecule or the binding of one aptamer affects the target's molecular interactions with other aptamers. Finally, it is important to note that our model, as with most previous models [12,13,15], assumes equilibrium mass-action kinetics. To extend the model, it may be desirable to introduce factors that break equilibrium at certain stages during selection to help accelerate the dissociation of weakly-bound aptamers, such as an active wash process.

## **Conclusion**

In this work, we have developed a model that enables experimentalists to determine selection conditions that will yield an optimally enriched aptamer pool after each round of a SELEX experiment based on two input parameters: background binding and initial bulk affinity distribution. While aptamers served as the main experimental system of our model, our approach can be applied with minor modification to virtually any bio-combinatorial library, including phage display, cell surface display and mRNA display, among others. The critical influence of target concentration and background binding in these display technologies would be equally important, and in experimental practice, similar trade-offs would be required to achieve ideal selection efficiencies.

## **Acknowledgements**

PJA acknowledges support from National Science Foundation CAREER Award 0956210. JFR appreciates final support from the UC RISE program at UCSB. JW and HTS acknowledge support from ARO Institute for Collaborative Biotechnologies, and the National Institutes of Health.

## References

1. Willis MC, Collins BD, Zhang T, Green LS, Sebesta DP, et al. (1998) Liposome-anchored vascular endothelial growth factor aptamers. *Bioconjugate chemistry* 9: 573–582. Available:<http://dx.doi.org/10.1021/bc980002x>. Accessed 21 July 2011.
2. Jellinek D, Green LS, Bell C, Lynott CK, Gill N, et al. (1995) Potent 2'-Amino-2'-deoxypyrimidine RNA Inhibitors of Basic Fibroblast Growth Factor. *Biochemistry* 34: 11363–11372. Available:<http://dx.doi.org/10.1021/bi00036a009>. Accessed 21 July 2011.
3. Plaxco KW, Soh HT (2011) Switch-based biosensors: a new approach towards real-time, in vivo molecular detection. *Trends in biotechnology* 29: 1–5. Available:[http://www.cell.com/trends/biotechnology/fulltext/S0167-7799\(10\)00179-4](http://www.cell.com/trends/biotechnology/fulltext/S0167-7799(10)00179-4). Accessed 21 July 2011.
4. Green LS, Jellinek D, Bell C, Beebe LA, Feistner BD, et al. (1995) Nuclease-resistant nucleic acid ligands to vascular permeability factor/vascular endothelial growth factor. *Chemistry & biology* 2: 683–695. Available:<http://www.ncbi.nlm.nih.gov/pubmed/9383475>. Accessed 21 July 2011.
5. Haller AA (1997) In vitro selection of a 7-methyl-guanosine binding RNA that inhibits translation of capped mRNA molecules. *Proceedings of the National Academy of Sciences* 94: 8521–8526. Available:<http://www.pnas.org/cgi/content/abstract/94/16/8521>. Accessed 21 July 2011.
6. Daniels DA, Chen H, Hicke BJ, Swiderek KM, Gold L (2003) A tenascin-C aptamer identified by tumor cell SELEX: systematic evolution of ligands by exponential enrichment. *Proceedings of the National Academy of Sciences of the United States of America* 100: 15416–15421. Available:<http://www.pnas.org/cgi/content/abstract/100/26/15416>. Accessed 21 July 2011.

7. Shangguan D, Li Y, Tang Z, Cao ZC, Chen HW, et al. (2006) Aptamers evolved from live cells as effective molecular probes for cancer study. *Proceedings of the National Academy of Sciences of the United States of America* 103: 11838–11843. Available:<http://www.pnas.org/cgi/content/abstract/103/32/11838>. Accessed 21 July 2011.
8. Bunka DHJ, Stockley PG (2006) Aptamers come of age - at last. *Nature reviews Microbiology* 4: 588–596. Available:<http://www.ncbi.nlm.nih.gov/pubmed/16845429>. Accessed 6 March 2012.
9. Ellington AD, Szostak JW (1990) In vitro selection of RNA molecules that bind specific ligands. *Nature* 346: 818–822. Available:<http://dx.doi.org/10.1038/346818a0>. Accessed 21 July 2011.
10. Tuerk C, Gold L (1990) Systematic evolution of ligands by exponential enrichment: RNA ligands to bacteriophage T4 DNA polymerase. *Science* 249: 505–510. Available:<http://www.sciencemag.org/content/249/4968/505.abstract>. Accessed 21 July 2011.
11. Ahmad KM, Oh SS, Kim S, McClellan FM, Xiao Y, et al. (2011) Probing the limits of aptamer affinity with a microfluidic SELEX platform. *PloS one* 6: e27051. Available:<http://www.pubmedcentral.nih.gov/articlerender.fcgi?artid=3215713&tool=pmcentrez&rendertype=abstract>. Accessed 12 March 2012.
12. Irvine D, Tuerk C, Gold L (1991) SELEXION. Systematic evolution of ligands by exponential enrichment with integrated optimization by non-linear analysis. *Journal of molecular biology* 222: 739–761. Available:<http://www.ncbi.nlm.nih.gov/pubmed/1721092>. Accessed 21 July 2011.
13. Vant-Hull B, Gold L, Zichi DA (2000) Theoretical principles of in vitro selection using combinatorial nucleic acid libraries. *Current protocols in nucleic acid chemistry* / edited by Serge L Beaucage [et al] Chapter 9: Unit 9.1.

- Available:<http://www.ncbi.nlm.nih.gov/pubmed/18428805>. Accessed 21 July 2011.
14. Vant-Hull B, Payano-Baez A, Davis RH, Gold L (1998) The mathematics of SELEX against complex targets. *Journal of molecular biology* 278: 579–597. Available:<http://www.ncbi.nlm.nih.gov/pubmed/9600840>. Accessed 28 September 2011.
  15. Levine HA, Nilsen-Hamilton M (2007) A mathematical analysis of SELEX. *Computational biology and chemistry* 31: 11–35. Available:<http://www.pubmedcentral.nih.gov/articlerender.fcgi?artid=2374838&tool=pmcentrez&rendertype=abstract>. Accessed 22 July 2011.
  16. Djordjevic M, Sengupta AM (2006) Quantitative modeling and data analysis of SELEX experiments. *Physical biology* 3: 13–28. Available:<http://www.ncbi.nlm.nih.gov/pubmed/16582458>. Accessed 15 July 2011.
  17. Sun F, Galas D, Waterman MS (1996) A mathematical analysis of in vitro molecular selection-amplification. *Journal of molecular biology* 258: 650–660. Available:<http://www.ncbi.nlm.nih.gov/pubmed/8636999>. Accessed 10 October 2011.
  18. Zhao Y, Granas D, Stormo GD (2009) Inferring binding energies from selected binding sites. *PLoS computational biology* 5: e1000590. Available:<http://dx.plos.org/10.1371/journal.pcbi.1000590>. Accessed 22 July 2011.
  19. Lou X, Qian J, Xiao Y, Viel L, Gerdon AE, et al. (2009) Micromagnetic selection of aptamers in microfluidic channels. *Proceedings of the National Academy of Sciences of the United States of America* 106: 2989–2994. Available:<http://www.pnas.org/cgi/content/abstract/106/9/2989>. Accessed 21 July 2011.